

## Accepted Article

**Title:** Tracking the Dynamic Folding and Unfolding of RNA G-Quadruplexes in Live Cells

**Authors:** Xiu-Cai Chen, Shuo-Bin Chen, Jing Dai, Jia-Hao Yuan, Tian-Miao Ou, Zhi-Shu Huang, and Jia-Heng Tan

This manuscript has been accepted after peer review and appears as an Accepted Article online prior to editing, proofing, and formal publication of the final Version of Record (VoR). This work is currently citable by using the Digital Object Identifier (DOI) given below. The VoR will be published online in Early View as soon as possible and may be different to this Accepted Article as a result of editing. Readers should obtain the VoR from the journal website shown below when it is published to ensure accuracy of information. The authors are responsible for the content of this Accepted Article.

**To be cited as:** *Angew. Chem. Int. Ed.* 10.1002/anie.201801999  
*Angew. Chem.* 10.1002/ange.201801999

**Link to VoR:** <http://dx.doi.org/10.1002/anie.201801999>  
<http://dx.doi.org/10.1002/ange.201801999>

## COMMUNICATION

## Tracking the Dynamic Folding and Unfolding of RNA G-Quadruplexes in Live Cells

Xiu-Cai Chen<sup>†</sup>, Shuo-Bin Chen<sup>†</sup>, Jing Dai, Jia-Hao Yuan, Tian-Miao Ou, Zhi-Shu Huang, and Jia-Heng Tan<sup>\*</sup>

**Abstract:** Due to the absence of methods for tracking RNA G-quadruplex dynamics, especially the folding and unfolding of this attractive structure in live cells, understanding of the biological roles of RNA G-quadruplexes is so far limited. Here we reported a new red-emitting fluorescent probe, **QUMA-1**, for a selective, continuous and real-time visualization of RNA G-quadruplexes in live cells. The applications of **QUMA-1** in several previously intractable applications, including live-cell imaging of the dynamic folding, unfolding and movement of RNA G-quadruplexes and visualizing the unwinding of RNA G-quadruplexes by RNA helicase have been demonstrated. Notably, our real-time results revealed the complexity of the dynamics of RNA G-quadruplexes in live cells. We anticipate that the further application of **QUMA-1** in combination with appropriate biological and imaging methods to explore the dynamics of RNA G-quadruplexes will uncover more information about the biological roles of RNA G-quadruplexes.

RNA can fold back on itself and form fully paired or non-canonically paired structures to execute diverse biological functions.<sup>[1]</sup> The mechanisms of many such processes in cells is still unknown because real-time in situ visualization of the folding and unfolding of RNA structures in cells is very difficult. Currently, only a few methods can be employed to directly examine RNA structures in cells and even fewer to examine non-canonically paired structures.<sup>[2]</sup>

One such structure is the RNA G-quadruplex that is formed upon self-assembly of guanine-rich RNA sequences into stacked G-quartets.<sup>[3]</sup> During the past decade, RNA G-quadruplexes have received a considerable amount of attention because of the biological significance of these structures.<sup>[4]</sup> The folding and unfolding of RNA G-quadruplex structures have been viewed as a biological on-off switch that may play vital roles in the regulation of a variety of cellular events.<sup>[5]</sup> For example, formation of G-quadruplexes in mRNAs may participate in the translational control. G-quadruplexes at telomeric RNA may regulate telomere elongation.<sup>[6]</sup> However, similar to the problems encountered while examining RNA structures, there is a lack of appropriate approaches to identify the dynamics of an RNA G-quadruplex structure in its native cellular context.

In previous cellular studies, imaging experiments using antibodies and molecular probes have supported the formation of RNA G-quadruplexes in cells;<sup>[7]</sup> however, more recent dimethyl sulfate (DMS) probing and reverse transcription (RT)-stop profiling studies have suggested that such structures are globally unfolded in the steady state.<sup>[8]</sup> These results made us curious about the nature of RNA G-quadruplex folding and unfolding in native cellular

contexts and about the factors that influence this dynamic process. Activatable fluorescent probes can potentially be used to answer these questions by lighting up RNA G-quadruplexes in live cells, whereas switching off upon the structures unfolding. However, few RNA G-quadruplex-specific fluorescent probes have been found, and none of these probes have been employed to track the dynamic folding and unfolding of RNA G-quadruplex structures in cells.<sup>[7b, 7c, 9]</sup> Obviously, a specific and applicable RNA G-quadruplex fluorescent probe is still in demand.

Here, we present a RNA G-quadruplex-specific fluorescent probe, **QUMA-1** (Figure 1A), and the application of this probe in the study of RNA G-quadruplex dynamics in cells. The scaffold of **QUMA-1** is the coumarin-hemicyanine fluorophore that was derived from our previously reported isaindigotone-based G-quadruplex probes.<sup>[10]</sup> This new compound was prepared via the condensation of a coumarin aldehyde and an N-methylated quinoline moiety (Scheme S1 and Figures S1–S13) and was identified as selectively staining RNA in HeLa cells by enzyme-digestion-based screening (Figure S14).

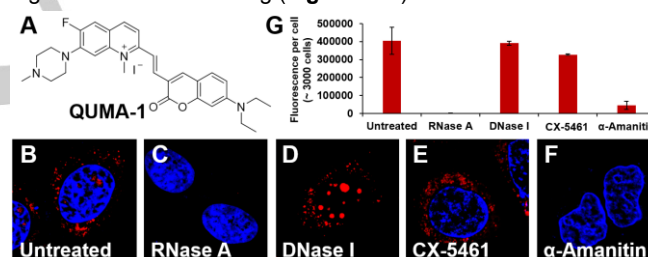


**Figure 1.** Illustration of the structure of **QUMA-1** and the specificity of **QUMA-1** for RNA in HeLa cells. (A) Chemical structure of **QUMA-1**. (B) Imaging of fixed cells stained with **QUMA-1**. (C) Complete loss of **QUMA-1** staining after RNase A treatment. (D) Maintenance of **QUMA-1** staining after DNase I treatment. (E) Maintenance of cytoplasmic, but not nuclear, **QUMA-1** staining after CX-5461 treatment. (F) Loss of cytoplasmic **QUMA-1** staining after  $\alpha$ -Amanitin treatment. (G) Quantification of the **QUMA-1** fluorescence intensity for B–F. For each sample, approximately 3000 cells were measured.

As shown in Figure 1B, the fixed HeLa cells stained by **QUMA-1** exhibited strong and distinct fluorescent foci. Most of these foci are located in cytoplasm, with a few in nucleoli (Figure S15). The specificity of **QUMA-1** for RNA was identified by the complete loss of the fluorescent signal upon treatment with RNase A (Figure 1C) but no loss of signal upon DNase I treatment (Figure 1D). To further validate the digestion results, we employed two RNA polymerase inhibitors, CX-5461 and  $\alpha$ -Amanitin, to inhibit the transcription of rRNA in nucleoli and RNA in cytoplasm, respectively.<sup>[11]</sup> The number of corresponding **QUMA-1** foci were significantly decreased upon the addition of the two inhibitors (Figures 1E–F). Similar results were observed upon quantification of cells using a high-content imaging platform (Figure 1G), further confirming the RNA specificity of **QUMA-1**.

We next asked what kind of RNAs will contribute to strong fluorescence signals of **QUMA-1** in cells. We therefore studied the fluorescence properties of **QUMA-1** with various RNAs (G-quadruplex, double stranded, single stranded, etc.) using fluorescence spectroscopy (Table S1 and Figures S16–S17). Notably, **QUMA-1** alone in buffer exhibited very weak emission, and only RNA G-quadruplexes (FMR1, TERRA, TB1 and MT3) could significantly enhance the fluorescence signal of **QUMA-1** at approximately 660 nm (Figure 2, Table S2, and Figures S18–

[\*] X.-C. Chen<sup>†</sup>, Dr. S.-B. Chen<sup>†</sup>, J. Dai, J.-H. Yuan, Prof. T.-M. Ou, Prof. Z.-S. Huang, and Prof. J.-H. Tan<sup>\*</sup>  
School of Pharmaceutical Sciences, Sun Yat-sen University  
Guangzhou 510006, China  
E-mail: tanjih@mail.sysu.edu.cn

[†] These authors contributed equally to this work.

Supporting information and the ORCID identification number(s) for the author(s) of this article can be found under:

## COMMUNICATION

**S20**).<sup>[12]</sup> Conversely, incubation of **QUMA-1** with these RNA G-quadruplexes in several G-quadruplex-unfolding conditions dramatically decreased the fluorescence signal (**Figure S21**). The  $K_D$  values of **QUMA-1** with the RNA G-quadruplex TERRA were up to 0.57  $\mu\text{M}$  (**Figure S22**), which corresponds to a much stronger affinity than that observed with the mutated single-stranded RNA TERRAmut ( $K_D > 5 \mu\text{M}$ ). In competition assays, the enhanced fluorescence due to the interactions of **QUMA-1** and RNA G-quadruplexes was only slightly affected in the presence of various amounts of competitive RNAs (**Figure S23**). Accordingly, these results showed that the activatable fluorescent probe **QUMA-1** preferentially recognizes G-quadruplex structures in vitro.

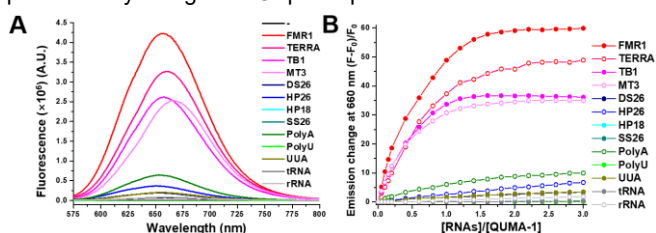


**Figure 2.** Fluorescence spectrum of **QUMA-1** with RNAs. (A) Fluorescence spectrum of 1  $\mu\text{M}$  **QUMA-1** with or without 2  $\mu\text{M}$  RNAs. (B) Fluorescence emission change of 1  $\mu\text{M}$  **QUMA-1** at 660 nm against the ratio of [RNAs]/[**QUMA-1**] at  $\lambda_{\text{ex}} = 555 \text{ nm}$ .

To further elucidate the cellular target of **QUMA-1**, we employed the chemical denaturant formamide and RNase III to destroy all RNA secondary structures and to specifically cleave double-stranded RNA, respectively. The formamide treatment led to a total loss of the **QUMA-1** foci (**Figure 3B**), but RNase III treatment did not affect the fluorescence signal (**Figure 3C**), suggesting that **QUMA-1** might selectively stain some kinds of non-canonically paired structure in HeLa cells. In contrast to cells treated with RNase III, cells treated with RNase T1 exhibited no **QUMA-1** foci (**Figure 3D**), and these results were the same as those observed with RNase A and formamide treatments. Since RNase T1 specifically cleaves RNA at guanosine residues, the loss of **QUMA-1** fluorescence might be a consequence of the degradation of RNA G-quadruplex structures. Accordingly, we individually transfected a FAM-labeled pre-folded RNA G-quadruplex and single-stranded RNA into cells to examine the interactions of these molecules with **QUMA-1**. Remarkably, the **QUMA-1** foci colocalized with the transfected RNA G-quadruplex instead of with the single-stranded RNA (**Figure S24**), showing that **QUMA-1** exhibits considerable selectivity for RNA G-quadruplexes.

Based on above observation, we then used a classical G-quadruplex ligand, BRACO19, and a RNA G-quadruplex-specific ligand, CarboxyPDS, to compete with **QUMA-1** for its endogenous cellular target. As shown in **Figures 3E–F**, the original fluorescence of **QUMA-1** in cells dramatically decreased after BRACO19/CarboxyPDS treatment (**Figure S25**).<sup>[7a, 13]</sup> On the other hand, unfolding of RNA G-quadruplexes using the C-rich oligonucleotide PolyC (**Figure 3G**) and overexpressed GFP-tagged G-quadruplex-specific RNA helicase DHX36 (**Figure 3H–I**) also resulted in a dramatic reduction in the number of **QUMA-1** foci.<sup>[14]</sup> Moreover, we employed two highly specific G-quadruplex antibodies, BG4 and D1,<sup>[7a, 15]</sup> in the immunofluorescence experiments to compare their localization with **QUMA-1** (**Figure 4** and **Figure S26**). As shown in **Figure 4**, the **QUMA-1** foci well colocalized with BG4 and D1 staining in the cytoplasm. Collectively, these results confirmed that **QUMA-1** can be used to selectively visualize RNA G-quadruplex structures in cells.

In addition to the performance of **QUMA-1**, we were also interested in its sensing mechanism. Interestingly, we found **QUMA-1** exhibited negligible fluorescence in low-viscosity buffer but strong fluorescence in high-viscosity glycerol solvent (**Figure S27A**). Since **QUMA-1** had little propensity to aggregate in buffer

solution (**Figure S28**), such enhancement may be caused by conformational changes in the excited state of **QUMA-1**, most likely by the rotation restriction around the methine-bridge that separates the coumarin and N-methylated quinoline moiety. This assumption was further supported by the correlation between fluorescence quantum yield and solvent viscosity (**Figure S27B**).<sup>[16]</sup> On the other hand, we also found the N-methylpiperazine group and the diethylamino-coumarin moiety in **QUMA-1** were both crucial for its high affinity and specificity to RNA G-quadruplex in cells, as revealed by a comparison with its structural analogs, **QUMA-2** and **QUID-1** (**Figure S14** and **Figure S29–S30**). The tight binding of **QUMA-1** to RNA G-quadruplexes instead of other RNA structures might lock **QUMA-1** in its fluorescent active conformation and activate the specific fluorescence accordingly.

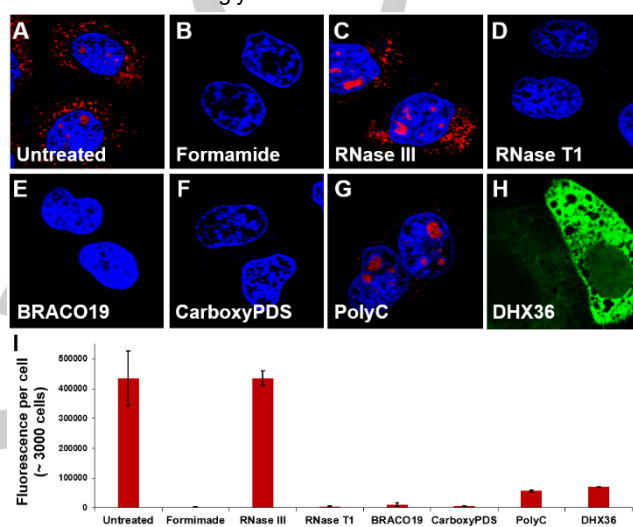


**Figure 3.** Illustration of the specificity of **QUMA-1** for RNA G-quadruplexes in HeLa cells. (A) Imaging of fixed cells stained with **QUMA-1**. (B) Complete loss of **QUMA-1** staining after formamide treatment. (C) Maintenance of **QUMA-1** staining after RNase III treatment. (D) Complete loss of **QUMA-1** staining after RNase T1 treatment. (E) Complete loss of **QUMA-1** staining after treatment with G-quadruplex ligand BRACO19. (F) Complete loss of **QUMA-1** staining after treatment with RNA G-quadruplex-specific ligand CarboxyPDS. (G) Loss of **QUMA-1** staining after treatment with C-rich sequence PolyC. (H) Loss of **QUMA-1** staining after overexpression of GFP-tagged G-quadruplex-specific RNA helicase DHX36. (I) Quantification of the **QUMA-1** fluorescence intensity for B–H. For each sample, approximately 3000 cells were measured.

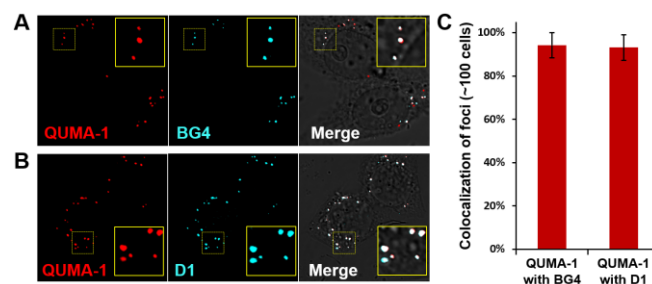


**Figure 4.** Illustration of the specificity of **QUMA-1** for RNA G-quadruplexes in HeLa cells. (A) Imaging of fixed cells stained with **QUMA-1** (red) and specific G-quadruplex antibody BG4 (cyan) after DNase I treatment. (B) Imaging of fixed cells stained with **QUMA-1** (red) and specific G-quadruplex antibody D1 (cyan) after DNase I treatment. (C) Quantification of **QUMA-1** foci inside specific G-quadruplex antibody foci. Enlarged image in the yellow box shows the colocalized foci. For each sample, approximately 100 cells were measured.

Encouraged by the outstanding specificity of **QUMA-1**, we sought to use this probe in live HeLa cells. We anticipated that **QUMA-1** fluorescence would be activated in the presence of RNA G-quadruplexes but would be quenched when the structures were unfolded. We could therefore track the dynamic changes in the RNA G-quadruplexes by analyzing the **QUMA-1** foci. To further

## COMMUNICATION

ensure the practicability of using **QUMA-1** in live cells, the cytotoxicity, photostability, response speed and cell permeability of **QUMA-1** were also determined and the probe was confirmed to be fully functional (Figures S31–S36).

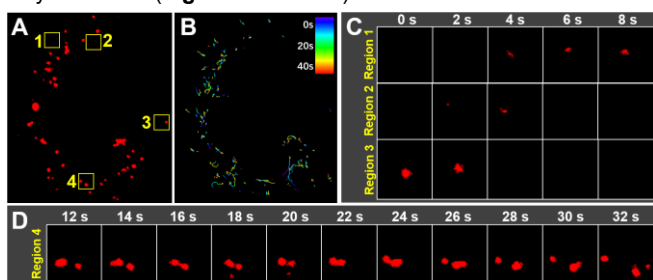


**Figure 5.** Tracking the dynamics of RNA G-quadruplexes by **QUMA-1** in live HeLa cells. (A) Imaging of live cells stained with **QUMA-1**. (B) Mobility analysis of the **QUMA-1** foci in A. (C, D) Time-lapse images of the region denoted by the boxes in A.

Upon **QUMA-1** treatment, the live HeLa cells exhibited strong and distinct foci, with a distribution similar to that in fixed cells (Figure 5A). Based on this observation, we next analyzed the movement and intensity of **QUMA-1** foci in a time-dependent experiment (Movie S1). The motion of **QUMA-1** foci could be mainly classified into three categories (Figure 5B and Figure S37): stationary, diffusive, and directed; these categories are consistent with previous mobility analyses of RNA molecules.<sup>[17]</sup> In addition, as expected, we found that some of the **QUMA-1** foci gradually disappeared during the observation period, while new fluorescent foci appeared (Figure 5C and Figure S38). This pattern of fluorescence change is indicative of a dynamic process of folding and unfolding of RNA G-quadruplexes in live cells. Moreover, we observed merge and split events of **QUMA-1** foci (Figure 5D), which might be attributed to assembly and disassembly of higher-order G-quadruplex structures or to large protein–G-quadruplex complexes.<sup>[18]</sup> Taken together, these continuous, real-time results revealed the complexity of the dynamics of RNA G-quadruplexes in live cells. The molecular probe **QUMA-1** potentially provides a promising tool for exploring the nature, mechanism and significance underlying such interesting dynamics.

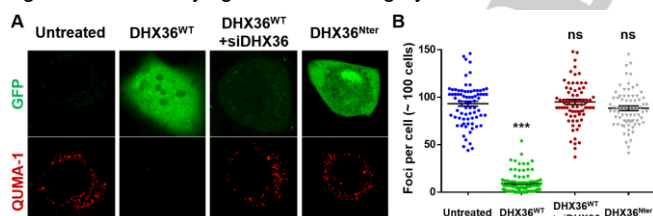


**Figure 6.** Tracking the dynamic folding and unfolding of RNA G-quadruplexes by **QUMA-1** in live HeLa cells with overexpressed, underexpressed GFP-tagged wild-type DHX36 ( $\text{DHX36}^{\text{WT}}$ ) and overexpressed GFP-tagged N-terminal recognition domain of DHX36 ( $\text{DHX36}^{\text{Nter}}$ ). For each sample, approximately 100 cells were measured. The data are expressed as the mean  $\pm$  SEM (standard error of mean): (\*\*\*)  $P < 0.0001$ , significantly different from the control; (ns) not significantly different from the control.

The study of changes in the folding and unfolding of RNA G-quadruplexes in native cellular contexts is crucial for understanding the biological significance of these structures. To further test the practicability of using **QUMA-1** to track such processes, GFP-tagged helicase DHX36 was used as a regulation factor to specifically unfold the RNA G-quadruplex structures. As shown in Figure 6A, overexpression of GFP-tagged DHX36 significantly decreased the fluorescence of **QUMA-1**, which was consistent with the results observed in fixed cells. Based on this observation, we next inhibited DHX36 expression using RNA interference to allow the refolding of the RNA G-quadruplexes. As anticipated, the fluorescence of **QUMA-1** was recovered, accompanied by a reduction in the levels of GFP-tagged DHX36

(Figure 6B and Figure S39). In addition, the fluorescence of **QUMA-1** was only slightly affected by the overexpression of N-terminal recognition domain of DHX36, whose core helicase domain was deleted, leading to the complete loss of unfolding activity. Therefore, these results provide an operational example of the practicability of using **QUMA-1** to track the dynamic folding and unfolding of RNA G-quadruplexes. Moreover, we envision the extended application of **QUMA-1** to identify unknown interactions between RNA G-quadruplexes and proteins in live cells.

In summary, we have successfully developed a new probe, **QUMA-1**, for the continuous, real-time visualization of the dynamics of RNA G-quadruplexes in live cells. **QUMA-1** is a selective and activatable fluorescent probe. Its fluorescence is significantly activated only by the RNA G-quadruplexes in cells, thus allowing us to carry out several previously intractable experiments, including live-cell imaging of the dynamic folding, unfolding and movement of RNA G-quadruplexes. Given the studies suggesting that RNA G-quadruplexes were folded in fixed cells but unfolded in steady state,<sup>[7a, 8]</sup> our real-time observations provide live cell-based dynamic evidence that has so far been absent in the field.

In this study, we also achieved live-cell imaging of the folding and unfolding processes of RNA G-quadruplexes by activating and inhibiting the G-quadruplex-specific RNA helicase DHX36. Proteins are key factors that are crucial in the regulation of the dynamics and subsequent biological functions of RNA G-quadruplexes. Previous studies also suggested the cell must find ways to get around the folding problem of RNA G-quadruplexes, and if given the opportunity, RNA G-quadruplexes will fold again.<sup>[7a, 8, 19]</sup> This is consistent with the dynamic change of RNA G-quadruplex structure revealed in our studies. Notably, the dynamics of RNA G-quadruplexes in live cells are very complex and need deeper understanding. We anticipate that the further application of **QUMA-1** in combination with modern biological and imaging methods to explore such attractive RNA G-quadruplex dynamics will uncover more information about the biological roles of RNA G-quadruplexes. The performance and feasibility of **QUMA-1** has promising potential in the future of understanding the nature of RNA G-quadruplexes. The discovery of **QUMA-1** and the collective results from this study may be an important step toward achieving this goal.

## Acknowledgements

This work was supported by the National Natural Science Foundation of China (21672268 and 81330077), the Natural Science Foundation of Guangdong Province (2015A030306004 and 2017A030308003), and Guangdong Provincial Key Laboratory of Construction Foundation (2011A060901014).

## Conflict of interest

The authors declare no conflict of interest.

**Keywords:** G-Quadruplexes • Fluorescent probes • Live-Cell imaging • RNA structures • Folding and unfolding

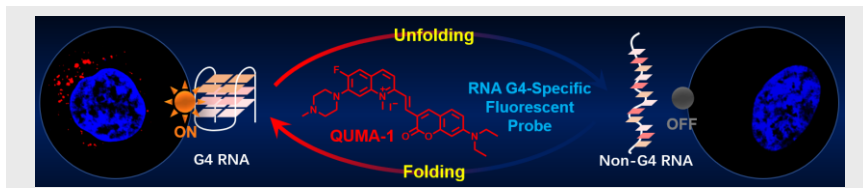
- [1] a) D. D. Licatalosi, R. B. Darnell, *Nat. Rev. Genet.* **2010**, *11*, 75–87; b) Y. Wan, M. Kertesz, R. C. Spitale, E. Segal, H. Y. Chang, *Nat. Rev. Genet.* **2011**, *12*, 641–655.
- [2] a) S. Rouskin, M. Zubradt, S. Washietl, M. Kellis, J. S. Weissman, *Nature* **2014**, *505*, 701–705; b) R. C. Spitale, R. A. Flynn, Q. C. Zhang, P. Crisalli, B. Lee, J. W. Jung, H. Y. Kuchelmeister, P. J.

## COMMUNICATION

- Batista, E. A. Torre, E. T. Kool, H. Y. Chang, *Nature* **2015**, *519*, 486-490; c) Y. Sugimoto, A. Vigilante, E. Darbo, A. Zirra, C. Militti, A. D'Ambrogio, N. M. Luscombe, J. Ule, *Nature* **2015**, *519*, 491-494; d) M. Gao, D. Gnutt, A. Orban, B. Appel, F. Righetti, R. Winter, F. Narberhaus, S. Muller, S. Ebbinghaus, *Angew. Chem. Int. Ed. Engl.* **2016**, *55*, 3224-3228; e) J. Tyrrell, J. L. McGinnis, K. M. Weeks, G. J. Pielak, *Biochemistry* **2013**, *52*, 8777-8785; f) M. J. Smola, T. W. Christy, K. Inoue, C. O. Nicholson, M. Friedersdorf, J. D. Keene, D. M. Lee, J. M. Calabrese, K. M. Weeks, *Proc. Natl. Acad. Sci. U. S. A.* **2016**, *113*, 10322-10327; g) J. L. McGinnis, Q. Liu, C. A. Lavender, A. Devaraj, S. P. McClory, K. Fredrick, K. M. Weeks, *Proc. Natl. Acad. Sci. U. S. A.* **2015**, *112*, 2425-2430.
- [3] G. W. Collie, S. M. Haider, S. Neidle, G. N. Parkinson, *Nucleic Acids Res.* **2010**, *38*, 5569-5580.
- [4] a) S. R. Wang, Q. Y. Zhang, J. Q. Wang, X. Y. Ge, Y. Y. Song, Y. F. Wang, X. D. Li, B. S. Fu, G. H. Xu, B. Shu, P. Gong, B. Zhang, T. Tian, X. Zhou, *Cell Chem. Biol.* **2016**, *23*, 1113-1122; b) A. Cammas, S. Millevoi, *Nucleic Acids Res.* **2016**, *45*, 1584-1595; c) C. K. Kwok, S. Balasubramanian, *Angew. Chem. Int. Ed. Engl.* **2015**, *54*, 6751-6754.
- [5] a) A. Bugaut, S. Balasubramanian, *Nucleic Acids Res.* **2012**, *40*, 4727-4741; b) S. Millevoi, H. Moine, S. Vagner, *Wiley Interdiscip. Rev. RNA* **2012**, *3*, 495-507; c) C. K. Kwok, A. B. Sahakyan, S. Balasubramanian, *Angew. Chem. Int. Ed. Engl.* **2016**, *55*, 8958-8961.
- [6] E. Cusanelli, C. A. Romero, P. Chartrand, *Mol. Cell.* **2013**, *51*, 780-791.
- [7] a) G. Biffi, M. Di Antonio, D. Tannahill, S. Balasubramanian, *Nat. Chem.* **2014**, *6*, 75-80; b) S. Xu, Q. Li, J. Xiang, Q. Yang, H. Sun, A. Guan, L. Wang, Y. Liu, L. Yu, Y. Shi, H. Chen, Y. Tang, *Nucleic Acids Res.* **2015**, *43*, 9575-9586; c) A. Laguerre, K. Hukezalie, P. Winckler, F. Katranji, G. Chanteloup, M. Pirrotta, J. M. Perrier-Cornet, J. M. Wong, D. Monchaud, *J. Am. Chem. Soc.* **2015**, *137*, 8521-8525; d) S.-B. Chen, M.-H. Hu, G.-C. Liu, J. Wang, T.-M. Ou, L.-Q. Gu, Z.-S. Huang, J.-H. Tan, *J. Am. Chem. Soc.* **2016**, *138*, 10382-10385.
- [8] J. U. Guo, D. P. Bartel, *Science* **2016**, *353*, 1382.
- [9] D. L. Ma, M. Wang, S. Lin, Q. B. Han, C. H. Leung, *Curr. Top. Med. Chem.* **2015**, *15*, 1957-1963.
- [10] J.-W. Yan, S.-B. Chen, H.-Y. Liu, W.-J. Ye, T.-M. Ou, J.-H. Tan, D. Li, L.-Q. Gu, Z.-S. Huang, *Chem. Commun.* **2014**, *50*, 6927-6930.
- [11] a) D. Drygin, A. Lin, J. Bliesath, C. B. Ho, S. E. O'Brien, C. Proffitt, M. Omori, M. Haddach, M. K. Schwaebe, A. Siddiqui-Jain, N. Streiner, J. E. Quin, E. Sanij, M. J. Bywater, R. D. Hannan, D. Ryckman, K. Anderes, W. G. Rice, *Cancer Res.* **2011**, *71*, 1418-1430; b) F. Brueckner, P. Cramer, *Nat. Struct. Mol. Biol.* **2008**, *15*, 811-818.
- [12] a) A. C. Blice-Baum, M. R. Mihailescu, *RNA* **2014**, *20*, 103-114; b) Y. Xu, K. Kaminaga, M. Komiyama, *J. Am. Chem. Soc.* **2008**, *130*, 11179-11184; c) V. T. Mukundan, A. T. Phan, *J. Am. Chem. Soc.* **2013**, *135*, 5017-5028; d) M. J. Morris, S. Basu, *Biochemistry* **2009**, *48*, 5313-5319.
- [13] a) M. Di Antonio, G. Biffi, A. Mariani, E. A. Raiber, R. Rodriguez, S. Balasubramanian, *Angew. Chem. Int. Ed. Engl.* **2012**, *51*, 11073-11078; b) A. M. Burger, F. Dai, C. M. Schultes, A. P. Reszka, M. J. Moore, J. A. Double, S. Neidle, *Cancer Res.* **2005**, *65*, 1489-1496.
- [14] a) M. C. Chen, P. Murat, K. Abecassis, A. R. Ferre-D'Amare, S. Balasubramanian, *Nucleic Acids Res.* **2015**, *43*, 2223-2231; b) N. M. Gueddouda, O. Mendoza, D. Gomez, A. Bourdoncle, J. L. Mergny, *Biochim. Biophys. Acta* **2017**, *1861*, 1382-1388.
- [15] H.-Y. Liu, Q. Zhao, T.-P. Zhang, Y. Wu, Y.-X. Xiong, S.-K. Wang, Y.-L. Ge, J.-H. He, P. Lv, T.-M. Ou, J.-H. Tan, D. Li, L.-Q. Gu, J. Ren, Y. Zhao, Z.-S. Huang, *Cell Chem. Biol.* **2016**, *23*, 1261-1270.
- [16] A. Granzhan, H. Ihmels, G. Viola, *J. Am. Chem. Soc.* **2007**, *129*, 1254.
- [17] a) H. Y. Park, H. Lim, Y. J. Yoon, A. Follenzi, C. Nwokafor, M. Lopez-Jones, X. Meng, R. H. Singer, *Science* **2014**, *343*, 422-424; b) C. Wang, B. Han, R. Zhou, X. Zhuang, *Cell* **2016**, *165*, 990-1001.
- [18] a) H. Kim, S. C. Abeyirigunawardena, K. Chen, M. Mayerle, K. Ragunathan, Z. Luthey-Schulten, T. Ha, S. A. Woodson, *Nature* **2014**, *506*, 334-338; b) H. L. Bao, T. Ishizuka, T. Sakamoto, K. Fujimoto, T. Uechi, N. Kenmochi, Y. Xu, *Nucleic Acids Res.* **2017**, *45*, 5501-5511.
- [19] S. B. Ramos, A. Laederach, *Nature* **2014**, *505*, 621-622.

## COMMUNICATION

## COMMUNICATION



**Dynamic folding and unfolding** of RNA G-quadruplexes in live cells have been demonstrated and discussed, by using a red-emitting, RNA G-quadruplex-specific, fluorescent probe, namely **QUMA-1**. The performance and feasibility of **QUMA-1** has promising potential in the future of understanding the nature of RNA G-quadruplexes.

Xiu-Cai Chen<sup>†</sup>, Shuo-Bin Chen<sup>†</sup>, Jing Dai, Jia-Hao Yuan, Tian-Miao Ou, Zhi-Shu Huang, and Jia-Heng Tan\*

Page No. – Page No.

**Tracking the Dynamic Folding and Unfolding of RNA G-Quadruplexes in Live Cells**

Accepted Manuscript